Theoretical and Experimental Insights Into Properties of Donor-σ-Acceptor Type Derivatives of Quinoxaline and Methanone Containing Different Donor Moieties

R. Keruckiene[1], M. Guzauskas[1], D. Volyniuk[1], V. E. Matulis[2], D. A. Lyakhov[3], J. V. Grazulevicius[1*]

[1]Department of Polymer Chemistry and Technology, Faculty of Chemical Technology, Kaunas University of Technology, K. Barsausko st. 59-500, Kaunas, Lithuania

[2]Belarusian State University, 4, Nezavisimosti avenue, 220030, Minsk, Republic of Belarus

[3]Computer, Electrical and Mathematical Science and Engineering Division, 4700 King Abdullah University of Science and Technology, Thuwal 23955-6900, Saudi Arabia

Table of Contents

Experimental

Instrumentation

^{1}H NMR spectra were recorded using a *Bruker Avance III* apparatus (400 MHz). The samples were prepared by dissolving around 20 mg of the material in 1 ml of deuterated chloroform ($CDCl_3$), acetone-d_6 or dimethylsulphoxide (DMSO-d_6). Hydrogen nuclei ^{1}H were excited by using the frequency of 400 MHz. The data is presented as chemical shifts (δ) in ppm (in parentheses: multiplicity, integration, coupling constant), in Fig. S1.

IR spectra were recorded by a *Vertex 70 Bruker* spectrometer equipped with an ATR attachment with a diamond crystal over frequencies of 600–3500 cm^{-1} with a resolution of 5 cm^{-1} over 32

* Corresponding author: juozas.grazulevicius@ktu.lt Department of Polymer Chemistry and Technology, Faculty of Chemical Technology, Kaunas University of Technology, K. Barsausko st. 59-450, Kaunas, Lithuania

scans. IR spectra are presented as a function of transparency (T) expressed in percent (%) against the wavenumber (v) expressed in cm^{-1}.

Mass spectra were obtained on a *Waters SQ Detector 2* mass spectrometer. The samples were prepared as diluted solutions of the compounds and were ionized by using electrospray ionization. Mass spectra are presented as an abundance of the ion versus the mass-to-charge ratio (m/z).

Absorption spectra of the dilute solutions (10^{-4}–10^{-5} mol/l) and thin films of the synthesized materials were recorded with a *Perkin Elmer Lambda 25* spectrophotometer.

Elemental analysis was performed using Exeter analytical ce-440 elemental analyzer.

Fluorescence spectra of the thin films and dilute solutions (10^{-4}–10^{-5} mol/l) of the synthesized compounds were recorded at room temperature with a luminescence spectrometer *Edinburgh Instruments FLS980*. Fluorescence quantum yields of the solutions and thin films of the materials were measured using an integrating sphere. Phosphorescence spectra of the solutions were recorded at 77 K. Fluorescence decays of the solid- state samples was conducted at 100 °C for 1 h.

Differential scanning calorimetry (DSC) measurements were carried out using a *TA Instruments Q2000* thermosystem. The samples were examined at a heating/cooling rate of 10 °C/min under nitrogen atmosphere.

Thermogravimetric analysis (TGA) was performed on a *TA Instruments Q50* analyser. The heating rate was 20 °C/min. The measurements were performed under nitrogen atmosphere.

Cyclic voltammetry measurements were performed using a glassy carbon working electrode (a disk with the diameter of 2 mm) in a three-electrode cell with an Autolab Type potentiostat – galvanostat. The measurements were carried out for the solutions in dry dichloromethane containing 0.1 M tetrabutylammonium hexafluorophosphate at 25 °C; the scan rate was 50 mV/s, the sample concentration was 10^{-3} M. The potentials were measured against silver as a reference

electrode. Platinum wire was used as a counter electrode. The potentials were calibrated with the standard ferrocene/ferrocenium (Fc/Fc^+) redox system[1].

The geometry and electronic structure of compounds **1**–**3** in ground and excited states were investigated within density functional theory using M062X[2], CAM-B3LYP[3] and B97XD[4] functionals with 6-31+G(d) basis set. The calculations were carried out in solution of toluene. Solvation effects were considered using the SMD model[5] in terms of Linear Response scheme[6]. Previously we have shown that the mentioned level of theory allows accurately reproduce electronic structure in ground and excited states of BODIPY dyes[7]. In the case of calculations of the absorption spectra, the geometry of the ground states S0 of compounds **1**–**3** was fully optimized in solution within DFT approach with subsequent calculation of the spectra within TD-DFT. For the calculations of photoluminescence spectra, the geometry of the first singlet excited state S1 was fully optimized in solution within TD-DFT. The calculated values of absorption and emission maxima were scaled using correlation equations from our previous paper[7] for better comparison with the experimental data. The corresponding correlation equations for each functional are given under the Tables 1, S1 and S2. Energy gap between the singlet and triplet states (ΔE_{S-T}) was calculated as energy difference between S1 and T1 excited states having the ground state geometry in toluene. All of the calculations were carried out using Gaussian16 program[8]. The analysis of electron density was performed using Multiwfn software[9].

Materials

2,4'-Bromophenacylbromide, 3,4-(diaminophenyl)phenylmethanone, phenothiazine, tetrabutylammonium bromide, sodium *tert*-butoxide, (purchased from Aldrich) bis(tri-*tert*-butylphosphine)palladium(0) (purchased from Fluorochem), 9,9-dimethyl-9,10-dihydroacridine (purchased from Center for Physical Sciences and Technology) were used as received. Thin layer chromatography was performed by using TLC plates covered with a silica gel matrix on aluminium backing (purchased from Aldrich).

(2-(4-Bromophenyl)quinoxalin-6-yl)phenylmethanone (**QM-Br**) was synthesised according to the reported procedure[10].

The following general procedure was used for the synthesis of target compounds. A mixture of **QM-Br** (1.29 mmol), corresponding donor fragment (1.36 mmol), either phenothiazine, dimethylacridan, or 3,6-di-*tert*-butylcarbazole, sodium *tert*-butoxide (2.58 mmol) were placed under vacuum into a Schlenk flask and backfilled with nitrogen three cycles before adding toluene (15 ml) and bis(tri-*tert*-butylphosphine)palladium(0) (10 w%). The reaction mixture was refluxed overnight. After cooling to room temperature, it was poured into water. The aqueous phase was extracted with dichloromethane (3 x 50 ml), and the combined organic phase was dried with sodium sulphate, filtered, and then the solvent was evaporated. The residue was purified by column chromatography on silica using ethylacetate:hexane mixture (1:1) as eluent.

(2-(4-(10H-Phenothiazin-10-yl)phenyl)quinoxalin-6-yl)(phenyl)methanone (**1**)

Yield of orange solid was 0.145 g (22%). MW=507g/mol. $C_{33}H_{21}N_3OS$. ^{1}H NMR (400 MHz, $CDCl_3$) δ 9.43 (s, 1H), 8.50 (s, 1H), 8.37 (d, *J* = 8.5 Hz, 2H), 8.27 (s, 1H), 7.91 (d, *J* = 7.4 Hz, 2H), 7.66 (t, *J* = 7.4 Hz, 2H), 7.53 (dd, J = 18.1, 10.1 Hz, 4H), 7.19 (d, *J* = 6.2 Hz, 2H), 7.01 (m, 5H), 6.68 (d, *J* = 8.1 Hz, 1H).

ATR-IR (solid state on ATR, cm^{-1}): 3059 (Ar. C–H), 2965 (Alk. C–H), 1459, 1442 (Alk. C=N), 1257 (Alk. C–N). MS: m/z 507 [M^+].

Elemental analysis of $C_{33}H_{21}N_3OS$ % Calc.: C, 78.08; H, 4.17; N, 8.28 % Found: C, 78.03; H, 4,21; N, 8.24.

(2-(4-(9,9-Dimethylacridan-10(9H)-yl)phenyl)quinoxalin-6-yl)(phenyl)methanone (**2**)

Yield of red solid was 0.150 g (23%). MW=517 g/mol. $C_{36}H_{27}N_3O$. ^{1}H NMR (400 MHz, DMSO) δ 9.81 (s, 1H), 8.60 (d, *J* = 8.5 Hz, 2H), 8.37 (s, 1 H), 8.18 (s, 1H), 7.82 (d, *J* = 7.4 Hz, 1H), 7.71 (d, *J* = 7.4 Hz, 1H), 7.66 (s, 1H), 7.5 (t, *J* = 7.4 Hz, 4H), 7.39 (s, 1H), 7.21 (d, *J* = 7.4 Hz, 1H), 7.0

(d, *J* = 7.4 Hz, 1H), 6.89 (s, 2H), 6.72 (s, 1H), 6.31 (d, *J* = 8.1 Hz, 2H), 6.19 (d, *J* = 8.1 Hz, 1H), 1.71 (d, *J* = 15.3 Hz, 6H).

ATR-IR (solid state on ATR, cm^{-1}): 3067 (Ar. C–H), 2967 (Alk. C–H), 1473, 1448 (Alk. C=N), 1268 (Alk. C–N). MS: m/z 517 [M^+].

Elemental analysis of $C_{36}H_{27}N_3O$ % Calc.: C, 83.53; H, 5.26; N, 8.12; % Found: C, 83.49; H, 5.30; N, 8.08.

(2-(4-(3,6-Di-*tert*-butyl-9H-carbazol-9-yl)phenyl)quinoxalin-6-yl)(phenyl)methanone (**3**)

Yield of dark red solid was 0.180 g (24%). MW=587 g/mol. $C_{41}H_{37}N_3O$. ^1H NMR (400 MHz, Acetone-d_6) δ 9.66 (s, 1H), 8.62 (d, *J* = 8.1 Hz, 2H), 8.33 (s, 2H), 8.18 (m, 4H), 7.82 (m, 3H), 7.61 (m, 2H), 7.52 (m, 3H), 7.49 (m, 4H), 1.46 (m, 18H).

ATR-IR (solid state on ATR, cm^{-1}): 3068 (Ar. C–H), 2965 (Alk. C–H), 1458(Alk. C=N), 1264 (Alk. C–N). MS: m/z 587 [M^+].

Elemental analysis of $C_{41}H_{37}N_3O$ % Calc.: C, 83.78; H, 6.35; N, 7.15; % Found: C, 83.82; H, 6.31; N, 7.11.

Figures and tables

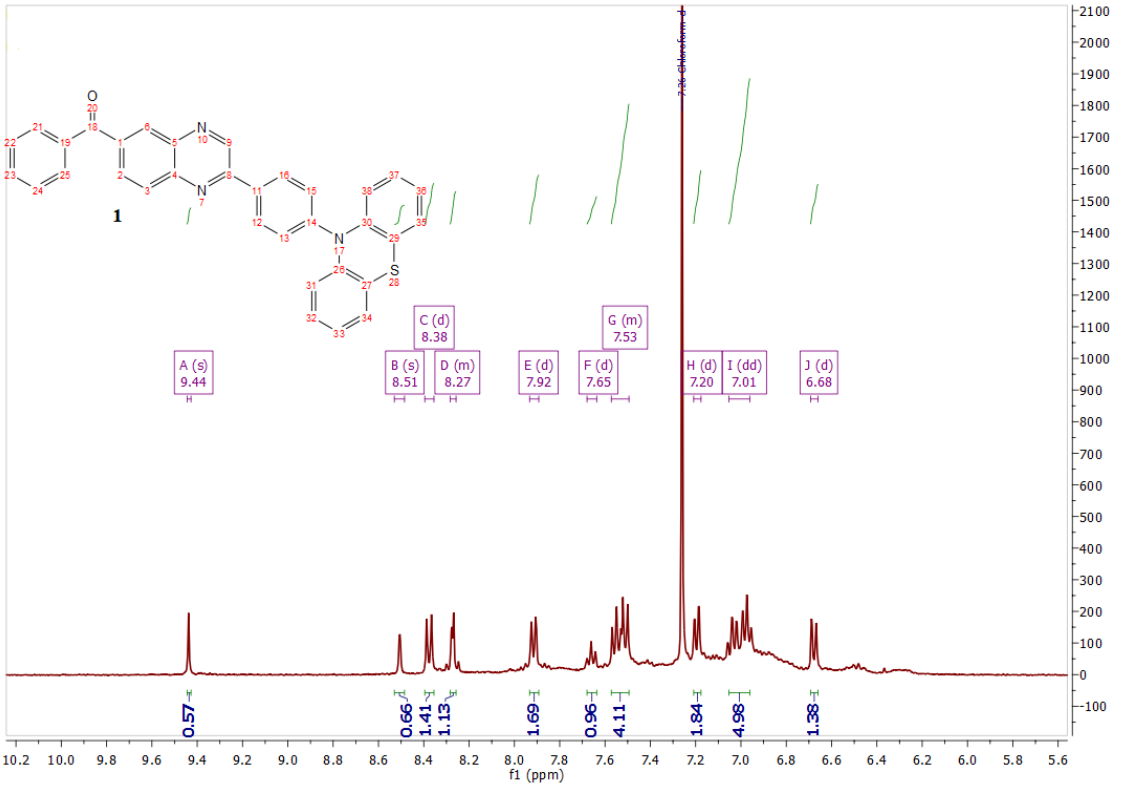

a)

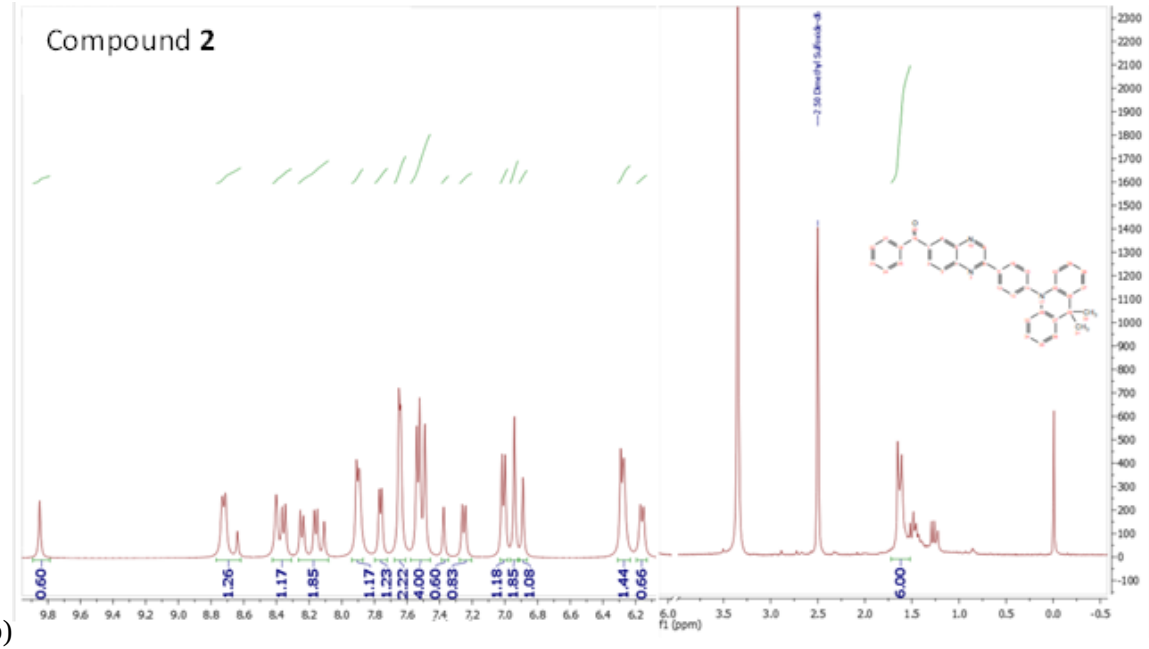

b)

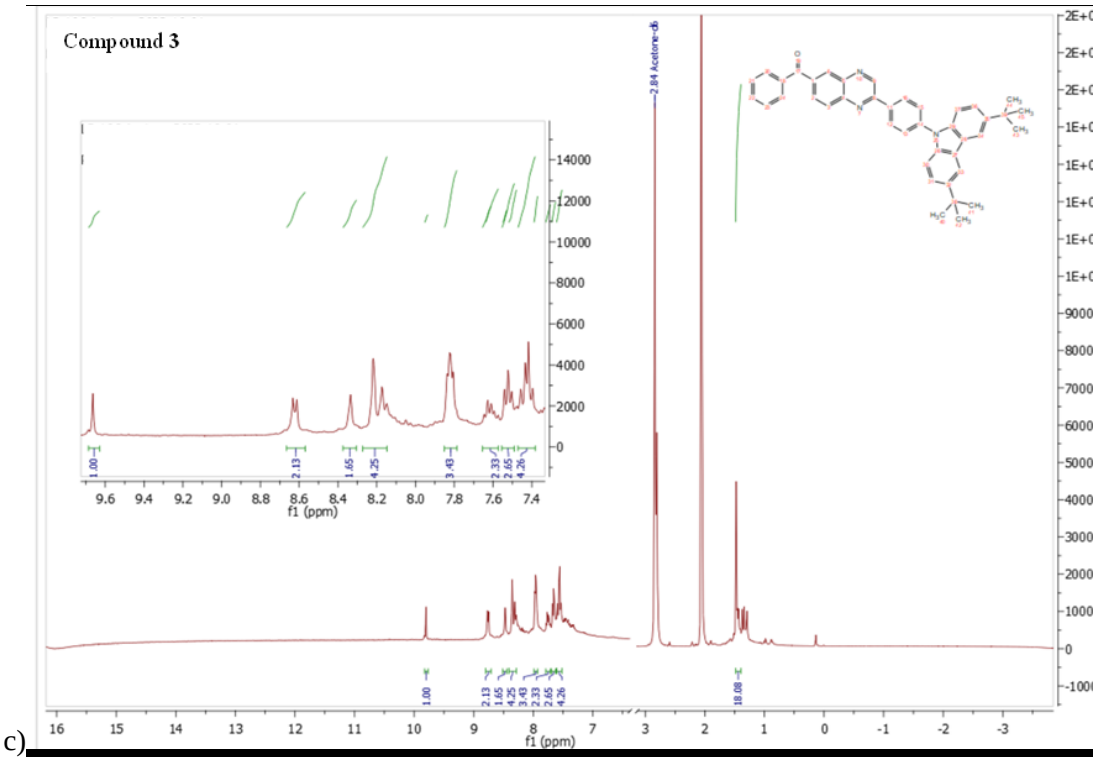

c)

Figure S1. ^{1}H NMR spectra of compounds **1** (in $CDCl_3$), **2** (in DMSO-d_6), and **3** (in acetone-d_6).

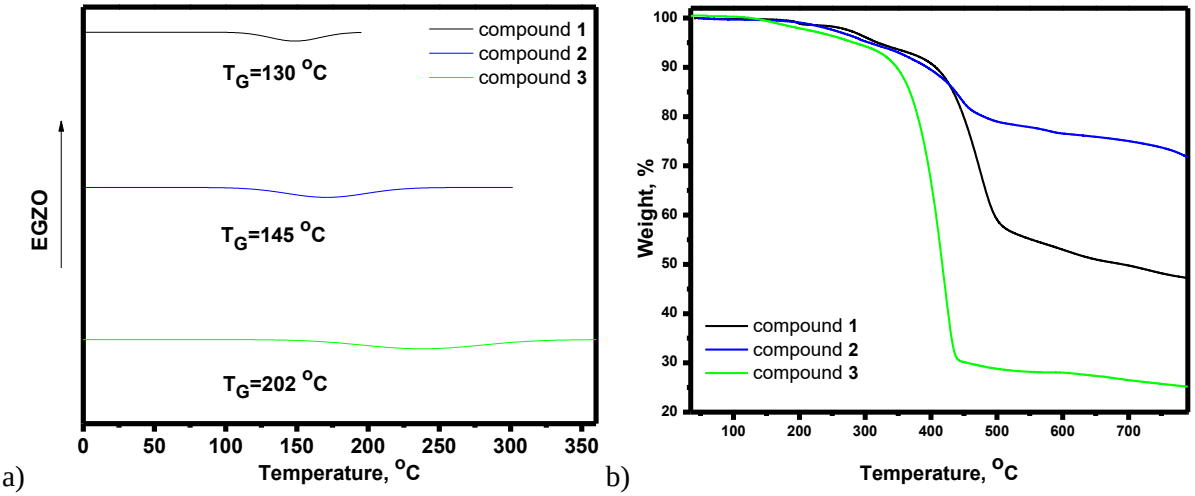

a) b)

Figure S2. DSC 2nd heating (a) and TGA (b) thermograms of compounds **1–3**. Scan rates 20 °C/min (TGA) and 10 °C/min (DSC).

As it can be seen from comparison of data of Tables 1 and S1 the results of calculations using M062X and CAM-B3LYP functionals are very close, except values of $\Delta E_{S\text{-}T}$. CAM-B3LYP functional overestimates the stability of triplet states and as a result overestimetes the values of $\Delta E_{S\text{-}T}$. Functional wB97XD gave inaccurate results of calculations for emission spectra as well as for charge transfer properties (Table S2). This inaccuracy caused by incorrect prediction of

electronic structure of S1 excited states of compounds **1**–**3** (see Figure S4 and c values in Table S2). Thus, according to wB97XD the largest coefficients in the CI expansion for S0→S1 excitation correspond to HOMO-8→LUMO (compounds **1** and **2**) or HOMO-7→LUMO (compound **3**) transitions, in contrast to the results of the other two functionals, according to which the largest coefficients in the CI expansion for all commpounds correspond to HOMO→LUMO transitions. As a result according to wB97XD S0→S1 transition for all compounds is a local excitation of quinoxaline moiety (Figure S4) which is not accompanied by significant dipole moment variation and characterized by negative values of τ-index. The fact that S0→S1 transition is a local transition in the acceptor fragment, which is the same for all three compounds, explains the almost identical values of λ_{ABS} and λ_{PL}, obtained using wB97XD functional. It should be noted, that in our previous studies[7,11–13], we showed that the results of wB97XD calculations are in good agreement with the experimental data, therefore inaccuracy observed in the present paper is rather unexpected.

Table S1. CAM-B3LYP/6-31+G(d) calculated wavelengths corresponding to the first (λ_{ABS}) absorption maxima, wavelengths corresponding to maxima in photoluminescence spectra (λ_{PL}), values of the largest coefficients in the CI expansion (c), oscillator strengths (f), dipole moments variation caused by electron excitation (Δμ), τ- and S_{+-}-indexes of compounds **1**–**3** and energy gaps between the singlet and triplet states (ΔE_{S-T}) in toluene.

Compound / Parameter	**1**	**2**	**3**
λ_{ABS}[a], nm	408	425	415
c	0.599 (HOMO→LUMO)	0.626 (HOMO→LUMO)	0.570 (HOMO→LUMO)
f	0.0008	$< 1 \cdot 10^{-4}$	0.9257
α, ^{0}	80	90	55
Δμ, Debye	27.257	29.347	20.270
τ-index	0.727	0.642	0.075
S_{+-}-index	0.749	0.742	0.841
ΔE_{S-T}, eV	1.20	1.02	1.15
λ_{PL}[a], nm	512	489	483
f	0.0002	0.5212	1.4315
α, ^{0}	90	67	42

[a] Scaled using correlation equation from our previous paper [4] values of λ_{ABS} and λ_{PL} are given: $\lambda_{ABS}(scaled) = 1.041 \cdot \lambda_{ABS}(calc.) + 58.40$; $\lambda_{PL}(scaled) = 0.712 \cdot \lambda_{PL}(calc.) + 187.21$.

Table S2. wB97XD/6-31+G(d) calculated wavelengths corresponding to the first (λ_{ABS}) absorption maxima, wavelengths corresponding to maxima in photoluminescence spectra (λ_{PL}), values of the largest coefficients in the CI expansion (c), oscillator strengths (f), dipole moments variation caused by electron

excitation (Δμ), τ- and S_{+-}-indexes of compounds **1**–**3** and energy gaps between the singlet and triplet states (ΔE_{S-T}) in toluene.

Compound / Parameter	**1**	**2**	**3**
λ_{ABS}[a], nm	403	403	402
c	0.591 (HOMO-8→LUMO)	0.499 (HOMO-8→LUMO)	0.420 (HOMO-7→LUMO)
f	0.0024	0.0080	0.0526
α, ^{0}	80	90	55
Δμ, Debye	1.010	2.736	1.097
τ-index	-1.599	-2.121	-1.670
S_{+-}-index	0.9778	0.974	0.965
ΔE_{S-T}, eV	1.11	1.11	1.14
λ_{PL}[a], nm	494	494	493
α, ^{0}	80	90	55

[a] Scaled using correlation equation from our previous paper [4] values of λ_{ABS} and λ_{PL} are given: $\lambda_{ABS}(scaled) = 1.062 \cdot \lambda_{ABS}(calc.) + 52.96$; $\lambda_{PL}(scaled) = 0.650 \cdot \lambda_{PL}(calc.) + 223.50$.

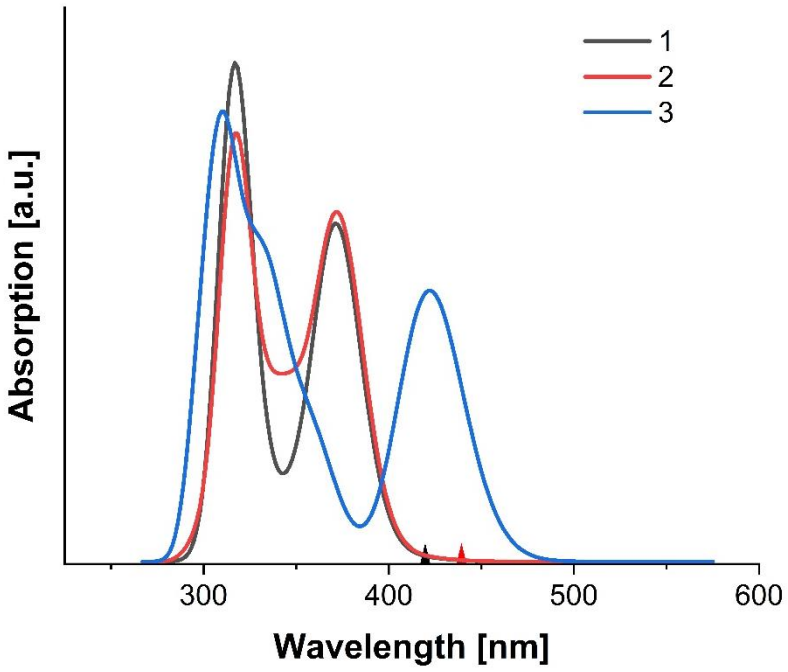

Figure S3. M062X/6-31+G(d) calculated scaled (using correlation equation from our previous paper[7]) absorption spectra of compounds **1**–**3** in toluene. The positions of the first calculated maxima in the spectra of compounds **1** and **2**, which characterized by very low intensity, are indicated by black and red riangles, respectively.

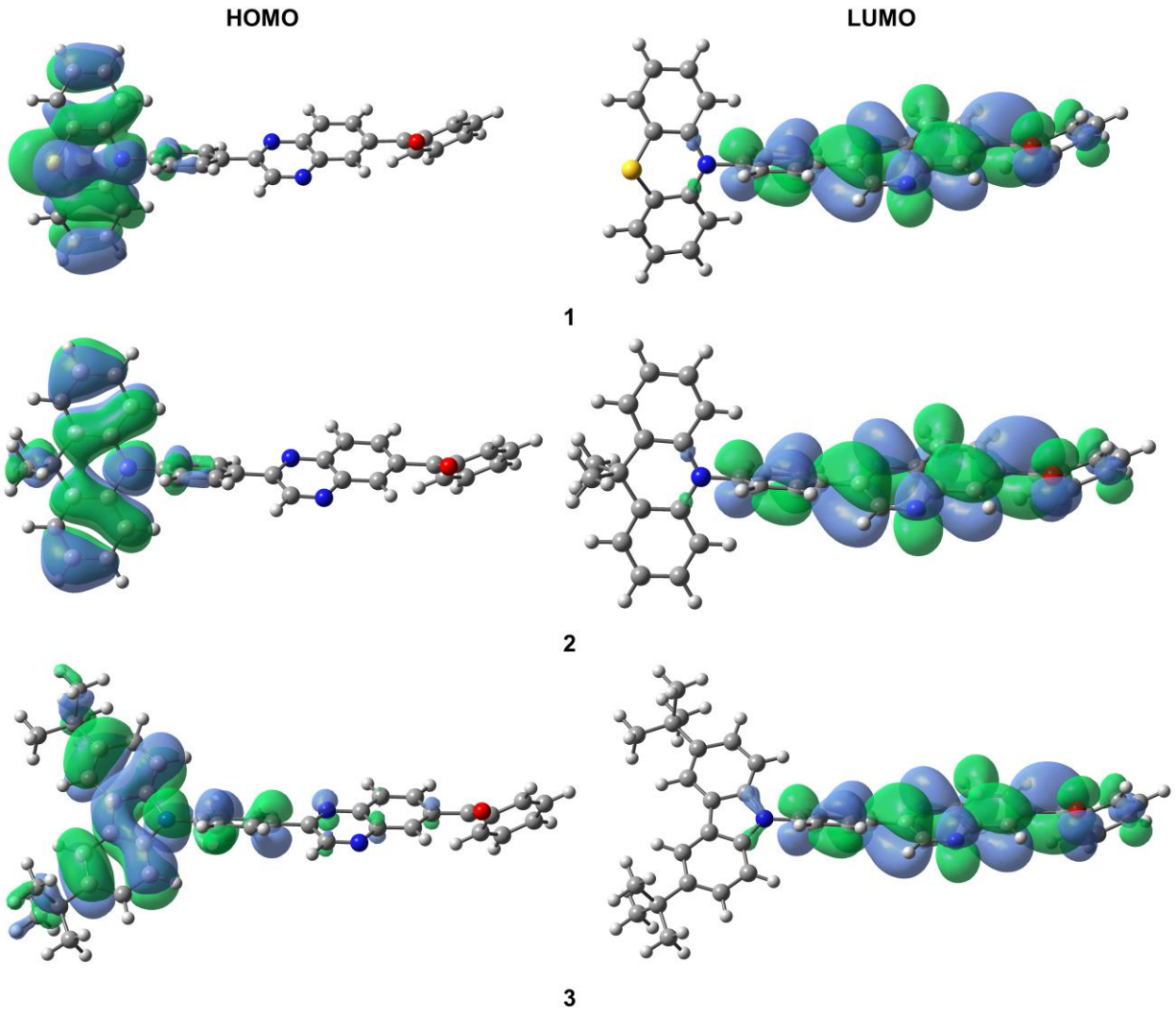

Figure S4. M062X/6-31+G(d) calculated plots of MOs of compounds **1–3** in toluene.

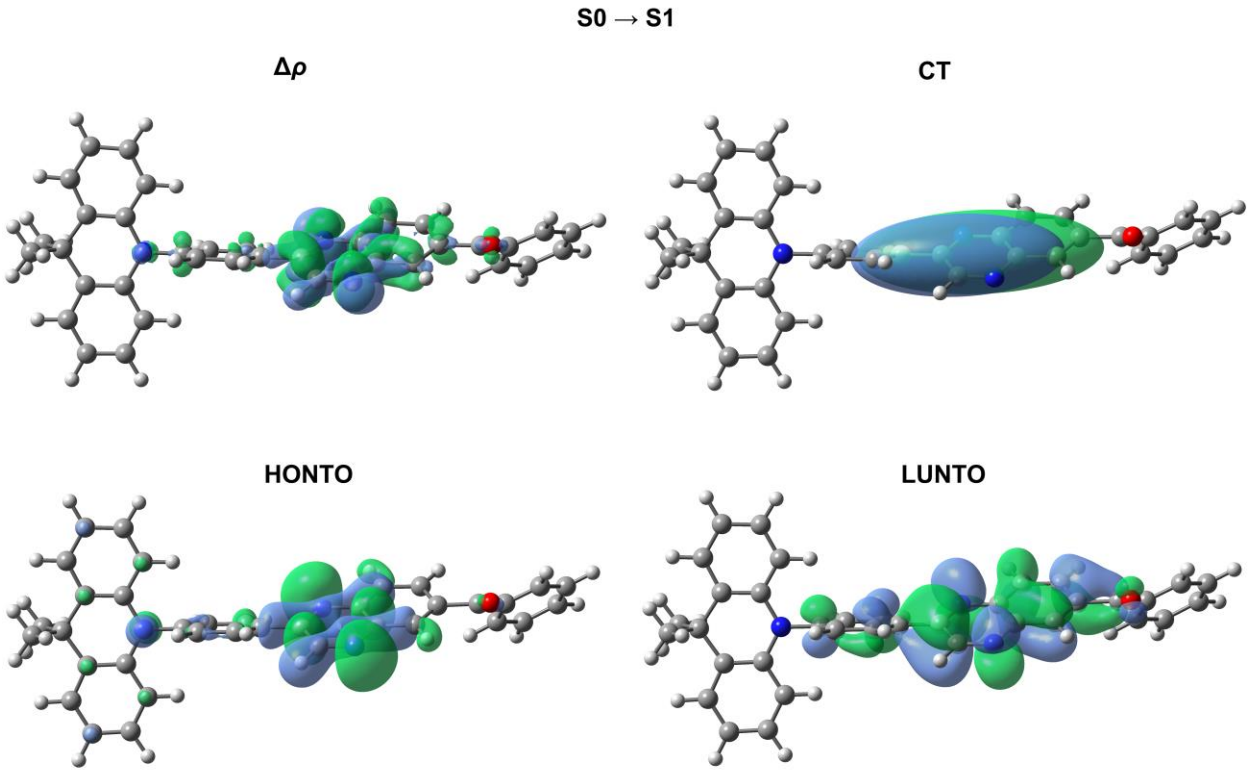

Figure S5. wB97XD/6-31+G(d) calculated plots of $\Delta\rho$ S1 – S0, S0→S1 CT and NTOs for compound **2** in toluene. Green (blue) regions indicate an increase (decrease) in ρ upon electronic transition.

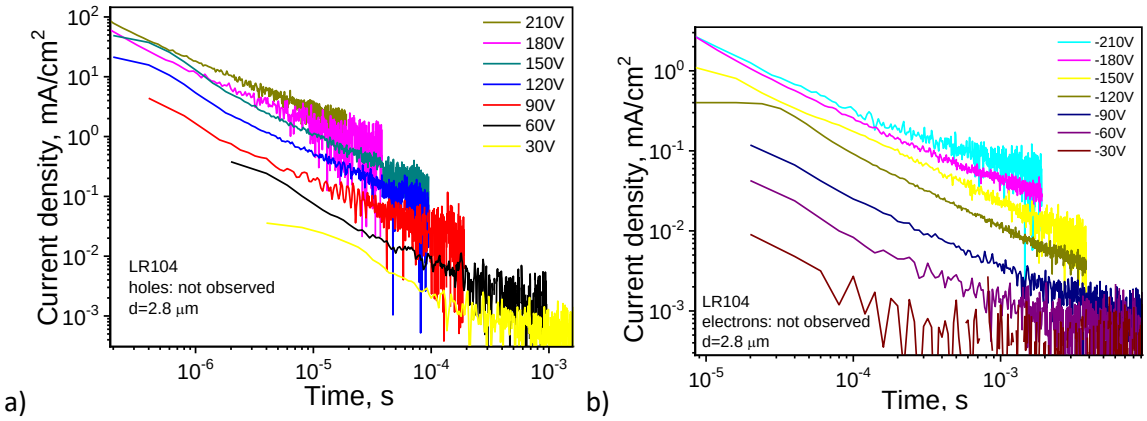

Figure S6. TOF signals for holes and electrons in vacuum-deposited layer of compound **1**.

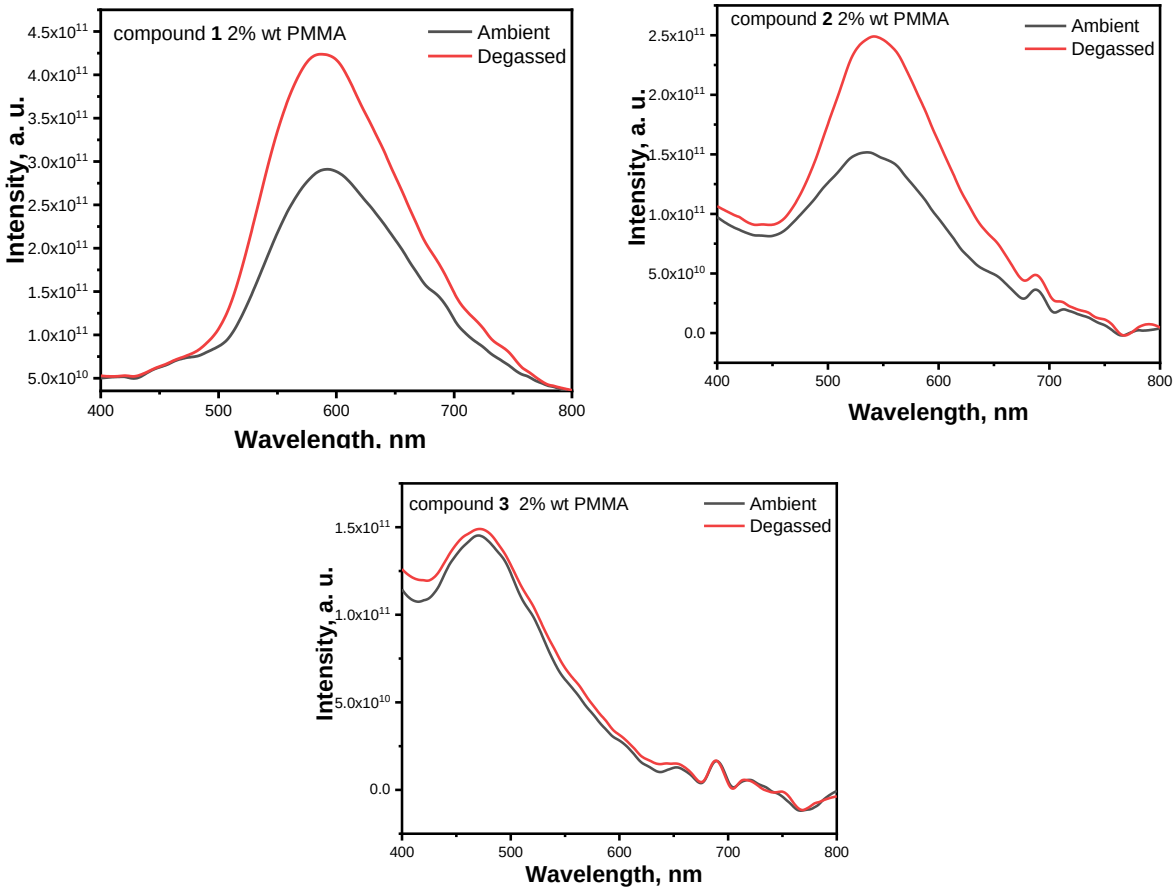

Figure S7. PL spectra of air-equilibrated and degassed solid samples of compounds doped PMMA matrix.

References

1 G. Gritzner and J. Kuta, *Pure Appl. Chem.*, 1984, **56**, 461–466.

2 Y. Zhao, D. G. Truhlar, Y. Zhao and · D G Truhlar, *Theor Chem Acc.*, 2008, **120**, 215–241.

3 T. Yanai, D. P. Tew and N. C. Handy, *Chem. Phys. Lett.*, 2004, **393**, 51–57.

4 J.-D. Chai and M. Head-Gordon, *J. Chem. Phys.*, 2008, **128**, 084106.

5 A. V. Marenich, C. J. Cramer and D. G. Truhlar, *J. Phys. Chem. B*, 2009, **113**, 6378–6396.

6 R. Cammi and B. Mennucci, *J. Chem. Phys.*, 1999, **110**, 5648.

7 V. E. Matulis, E. G. Ragoyja, O. A. Ivashkevich and C. E. Vitaly Matulis, *Int J Quantum Chem*, 2020, **120**, 26159.

8 M. J. Frisch, G. W. Trucks, H. B. Schlegel, G. E. Scuseria, M. A. Robb, J. R. Cheeseman, G. Scalmani, V. Barone, G. A. Petersson, H. Nakatsuji, X. Li, M. Caricato, A. Marenich, J. Bloino, B. G. Janesko, R. Gomperts, B. Mennucci, H. P. Hratchian, J. V. Ortiz, A. F. Izmaylov, J. L. Sonnenberg, D. Williams-Young, F. Ding, F. Lipparini, F. Egidi, J. Goings, B. Peng, A. Petrone, T. Henderson, D. Ranasinghe, V. G. Zakrzewski, J. Gao, N. Rega, G. Zheng, W. Liang, M. Hada, M. Ehara, K. Toyota, R. Fukuda, J. Hasegawa, M. Ishida, T. Nakajima, Y. Honda, O. Kitao, H. Nakai, T. Vreven, K. Throssell, J. J. A. Montgomery, J. E. Peralta, F. Ogliaro, M. Bearpark, J. J. Heyd, E. Brothers, K. N. Kudin, V. N. Staroverov, T. Keith, R. Kobayashi, J. Normand, K. Raghavachari, A. Rendell, J. C. Burant, S. S. Iyengar, J. Tomasi, M. Cossi, J. M. Millam, M. Klene, C. Adamo, R. Cammi, J. W. Ochterski, R. L. Martin, K. Morokuma, O. Farkas, J. B. Foresman and D. J. Fox, *Gaussian, Inc. Wallingford CT*.

9 T. Lu and F. Chen, *J. Comput. Chem.*, 2012, **33**, 580–592.

10 J. Liang, C. Li, Y. Cui, Z. Li, J. Wang and Y. Wang, *J. Mater. Chem. C*, 2020, **8**, 1614–1622.

11 R. Keruckiene, N. Kusas, L. Dvylys, E. Skuodis, V. E. Matulis, E. G. Ragoyja, D. A. Lyakhov, I. Klymenko and J. V. Grazulevicius, *J. Lumin.*, , DOI:10.1016/J.JLUMIN.2021.118502.

12 J.-D. Chai and M. Head-Gordon, *J. Chem. Phys.*, 2008, **128**, 084106.

13 N. Masimukku, D. Gudeika, D. Volyniuk, O. Bezvikonnyi, J. Simokaitiene, V. Matulis, D. Lyakhov, V. Azovskyi, J. Vidas and G. Ulevič, *Phys. Chem. Chem. Phys*, 2022, **5070**, 5070.